

# Intracardiac flow dynamics in mitral regurgitation: state of the art

**Lorenzo Serio** <sup>1</sup>, **Riccardo Beccari** <sup>1</sup>, **Stefano Nistri**<sup>1,2</sup>, **Antonella Cecchetto** <sup>1</sup>, **Gianni Pedrizzetti** <sup>3</sup>, and **Donato Mele** <sup>1,\*</sup>

<sup>1</sup>Department of Cardiac Thoracic Vascular Sciences and Public Health, University of Padova, Via Giustiniani, 2, 35128 Padova, Italy

<sup>2</sup>Cardiology Service, CMSR Veneto Medica, Via Vicenza 204, 36077 Altavilla Vicentina (VI), Italy

<sup>3</sup>Department of Engineering and Architecture, University of Trieste, Trieste, Italy

Received 31 December 2024; accepted after revision 6 February 2025; online publish-ahead-of-print 19 February 2025

## Abstract

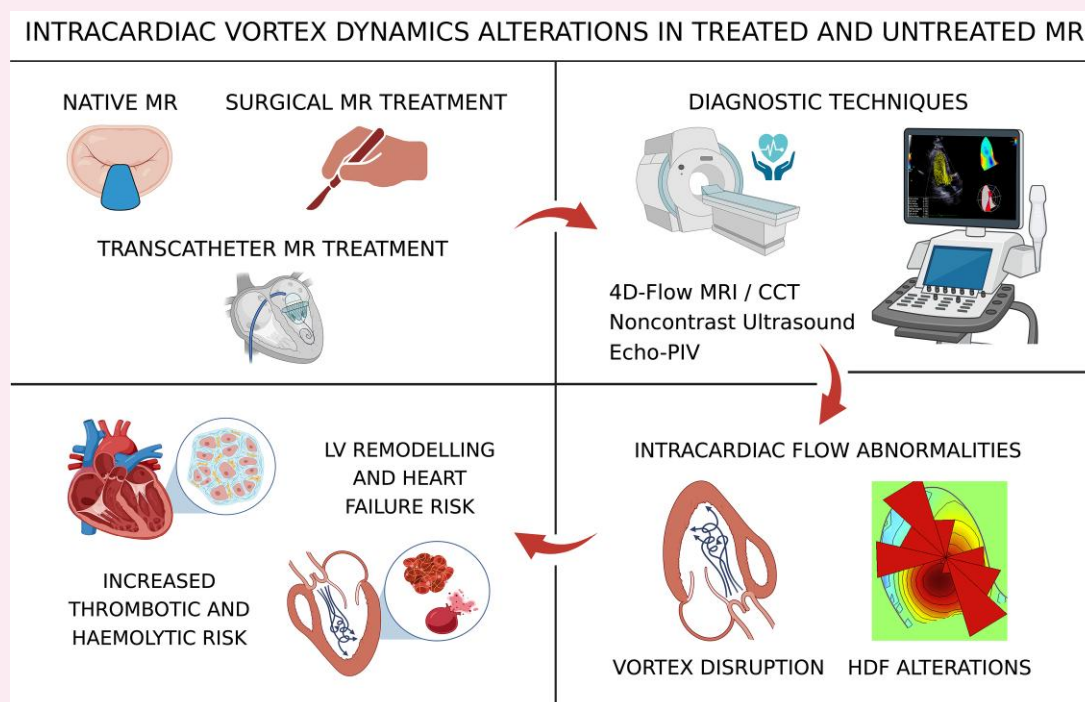
Intracardiac flow dynamics is a complex phenomenon interrelated with cardiac mechanics. Today, it can be evaluated non-invasively using various imaging modalities, including echocardiography, magnetic resonance imaging, and computed tomography. This review explores the effects of mitral regurgitation on blood flow dynamics inside the left ventricular and atrial cavities and emphasizes the disruption of normal flow dynamics caused by mitral regurgitation, leading to turbulent flow and increased energy dissipation. It further examines the consequences of mitral valve repair and replacement, noting that, while repair generally improves intracardiac flow dynamics compared with replacement, residual flow disturbances may persist. Finally, the implications of abnormal intracardiac vorticity on left ventricular wall stress, myocardial remodelling, and thromboembolic risk are discussed.

\* Corresponding author: E-mail: [donato.mele@unipd.it](mailto:donato.mele@unipd.it)

© The Author(s) 2025. Published by Oxford University Press on behalf of the European Society of Cardiology.

This is an Open Access article distributed under the terms of the Creative Commons Attribution-NonCommercial License (<https://creativecommons.org/licenses/by-nc/4.0/>), which permits non-commercial re-use, distribution, and reproduction in any medium, provided the original work is properly cited. For commercial re-use, please contact [reprints@oup.com](mailto:reprints@oup.com) for reprints and translation rights for reprints. All other permissions can be obtained through our RightsLink service via the Permissions link on the article page on our site—for further information please contact [journals.permissions@oup.com](mailto:journals.permissions@oup.com).

## Graphical Abstract



CCT, cardiac computed tomography; HDF, haemodynamic force; LV, left ventricle; MR, mitral regurgitation; MRI, magnetic resonance imaging; PIV, particle imaging velocimetry.

## Keywords

mitral regurgitation • intracardiac flow dynamics • cardiac vortex

## Introduction

The intricate study of intracardiac flow dynamics has garnered significant attention over the past decade, greatly enhancing our understanding of various cardiovascular conditions, particularly concerning disease mechanisms, treatment effects, and clinical outcomes.<sup>1,2</sup>

Mitral regurgitation (MR) is typically assessed for its complex haemodynamic implications and its impact on systolic left ventricle (LV) function. However, detailed analyses of intracardiac flow dynamics in patients with MR have documented flow alterations associated with this condition and their negative consequences. Additionally, studies of blood flow dynamics have been conducted in patients who have undergone surgical and percutaneous interventions for severe MR. While these corrective treatments are effective in alleviating symptoms and restoring haemodynamic parameters, they can also lead to significant changes in physiological flow patterns. Such alterations may increase wall stress and energy dissipation within the heart, potentially influencing disease progression and the occurrence of complications.

This review aims to synthesize the current preclinical and clinical evidence regarding changes in intracardiac flow dynamics in MR patients, both before and after corrective interventions. By elucidating the role of these flow alterations, we seek to clarify their implications for adverse effects and to inform diagnostic and therapeutic strategies in the management of MR.

## Techniques for assessing intracardiac flow dynamics

Non-invasive assessment of intracardiac flow dynamics can be achieved through various imaging modalities, primarily echocardiography and

magnetic resonance imaging (MRI) (Figure 1). A detailed description of these techniques, with their advantages and limitations, is available elsewhere.<sup>1</sup>

Echocardiography can be combined with contrast studies to facilitate particle image velocimetry (PIV) for the assessment of intracardiac flow dynamics. This assessment can also be obtained by processing colour Doppler images.<sup>1,2</sup> Commercially available colour Doppler-based techniques include vector flow mapping (VFM)<sup>1</sup> and HyperDoppler.<sup>3</sup>

Since intraventricular flow is a three-dimensional (3D) phenomenon, assessing the flow in 3D would be ideal. However, 3D colour Doppler-based techniques are not currently available for clinical application. The optimal two-dimensional (2D) imaging plane to analyse flow dynamics inside the LV cavity is the apical long-axis view in transthoracic echocardiography, as it allows for imaging of the maximum intraventricular area, including both the inflow and outflow tracts.

MRI enables 3D volume acquisition with velocity parameters encoded in three spatial directions using four-dimensional (4D) time-resolved phase-contrast imaging, commonly referred to as 4D-flow MRI.<sup>1</sup>

Cardiac computed tomography (CCT) does not inherently measure flow quantities such as blood velocity or pressure. However, recent advances have integrated it with computational fluid dynamics, resulting in 4D-flow CCT.<sup>4</sup>

## Physiological intracardiac flow patterns

### Left ventricle

Under physiological conditions, transmitral diastolic blood flow generates a vortex ring inside the LV cavity, which has a toroidal shape.<sup>5</sup> This

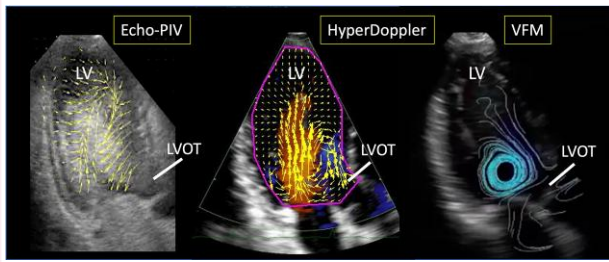


**Figure 1** Example of a LV long-axis view obtained using different cardiac ultrasound techniques for assessment of intracardiac flow dynamics. In each panel, rotation of blood flow inside the LV cavity is visualized. Echo-PIV, echocardiographic particle imaging velocimetry; LV, left ventricle; LVOT, left ventricular outflow tract; VFM, vector flow mapping.

process begins as blood moves from the left atrium (LA) into the LV, creating a shear layer at the trailing edge of the anterior and posterior mitral valve (MV) leaflets.

In the echocardiographic apical long-axis view, two distinct vortex components can be observed: a primary clockwise vortex beneath the anterior mitral leaflet (AML) and a smaller, transient counterclockwise vortex beneath the posterior mitral leaflet (PML) (Figure 2). The posterior vortex dissipates rapidly, while the anterior vortex expands and re-directs blood towards the left ventricular outflow tract (LVOT). During systole, the intraventricular pressure gradient (IVPG) reverses, propelling blood from the apex to the LVOT.

This vortex system facilitates the seamless transformation of incoming diastolic flow into upward systolic outflow, aligning haemodynamic forces along the longitudinal axis of the LV throughout the cardiac cycle.<sup>6</sup> The distribution and intensity of the LV haemodynamic forces can be visualized in polar histograms (Figure 3).

The formation of vortices minimizes the dissipation of kinetic energy (KE), thus enhancing systolic ejection and optimizing myocardial bioenergetics. Furthermore, the continuous washout effect along the trabeculated inner wall of the LV helps prevent thrombus formation and supports effective closure of AML during late diastole. The asymmetric structure of the MV leaflets governs these dynamics.<sup>7</sup>

## Left atrium

Vortical flow is the physiological flow pattern in the LA cavity<sup>8</sup> (Figure 4). This flow primarily originates from the high-velocity blood entering through the left pulmonary veins, colliding with the inflow from the other pulmonary veins. A distinct vortex near the inflow from the left pulmonary veins during both systole and diastole has been demonstrated in normal subjects.<sup>9,10</sup>

The vortex flow pattern plays a crucial role in preventing blood stasis in the LA cavity while preserving KE. Enlargement of LA volume correlates significantly with attenuation of vortex flow patterns.<sup>10</sup>

## Measures of intracardiac flow dynamics

Several quantitative parameters for characterizing vortex flow properties have been reported<sup>1,2</sup> (Table 1). Some measures are geometric, such as the vortex area, length, and depth, while others are temporal parameters, such as the vortex formation time. There are also measures that express vorticity, vortex circulation, and intensity; they can

be positive or negative depending on the direction of blood flow (negative for clockwise flow and positive for counterclockwise flow). Energetic properties include KE, kinetic energy loss (kEL) or dissipation (kED), and kinetic pressure (KP). Energy measures can vary with age.<sup>11</sup> The so-called turbulent KE (tKE) is a direction-independent measure of the intensity of turbulence in a flow.

Additional evaluations reflect the IVPG, specifically its intensity during the different phases of the heart cycle or its deviation from the axial direction.<sup>12</sup> In addition, different types of shear stress can be calculated, such as wall shear stress (WSS), viscous shear stress (VSS), and Reynolds shear stress (RSS). RSS is generally taken as a metric for the effect of turbulence.

Measures of intracardiac flow dynamics can be expressed as the mean value throughout the cardiac cycle or can be evaluated during specific phases of the cycle (for example, during LV early filling, late filling, or systole). They can be represented using specific units or as dimensionless ratios (for example, indexing a vortex property to its value within the entire cardiac chamber).

## Native MR

### Left ventricle

Gooden *et al.*<sup>13</sup> in an in vitro study showed that severe MR was characterized by an increase in LV inflow peak velocity, a high vorticity throughout diastole, and an increase in maximum RSS at peak flow. Alterations were more pronounced in the antero-posterior plane compared with the commissural plane.

Pilla *et al.*<sup>14</sup> in an animal model of ischaemic MR induced by a posterolateral myocardial infarction observed a significant delay in peak vortex formation compared with control animals.

Obermeier *et al.*<sup>15</sup> described two representative cases of severe MR (one with an LV aneurysm) in which no clear ring vortex structure evolved during diastolic inflow. Moreover, the early diastolic inflow jet was decomposed over the course of diastole, resulting in an unstructured flow. Higher kED was observed compared with patients without MR.

Al-Wakeel *et al.*<sup>16</sup> reported higher non-normalized mean KE, early diastolic, and late diastolic peak KE values in patients with MR compared with healthy individuals. However, when the KE was normalized relative to LV blood volume, these differences were no longer significant. In patients with MR, a larger fraction of recirculating blood was detectable, along with individual patterns of vortices scattered around the LV.

Wang *et al.*<sup>17</sup> in patients with degenerative MR (DMR) mostly due to PML prolapse, observed that diastolic kEL was elevated compared with normal control subjects, likely due to the more powerful collisions of filling flow with LV walls. Diastolic kEL has been reported to increase with the severity of MR.

Pugliese *et al.*<sup>18</sup> evidenced that in DMR a normal diastolic vorticity was maintained, with two counter-rotating vortices in the apical long-axis view, although systolic ejection was disrupted by multiple clockwise vortices localized around the MV. In contrast, functional MR (FMR) patients exhibited a single clockwise vortex during early diastolic filling, with systolic flow directing blood towards both the LVOT and LA, forming a counterclockwise vortex near the MV.

Filomena *et al.*<sup>19</sup> in patients with severe MR (60% with ischaemic aetiology) observed a negative value of the vortex intensity index, reflecting a clockwise rotation of the blood flow. Interestingly, vortex area index, intensity index, and kED index were higher compared with values observed in normal subjects in a different investigation.<sup>20</sup>

### Left atrium

Dyverfeldt *et al.*<sup>10</sup> examined patients with PML prolapse and eccentric MR jets directed towards the interatrial septum and observed the

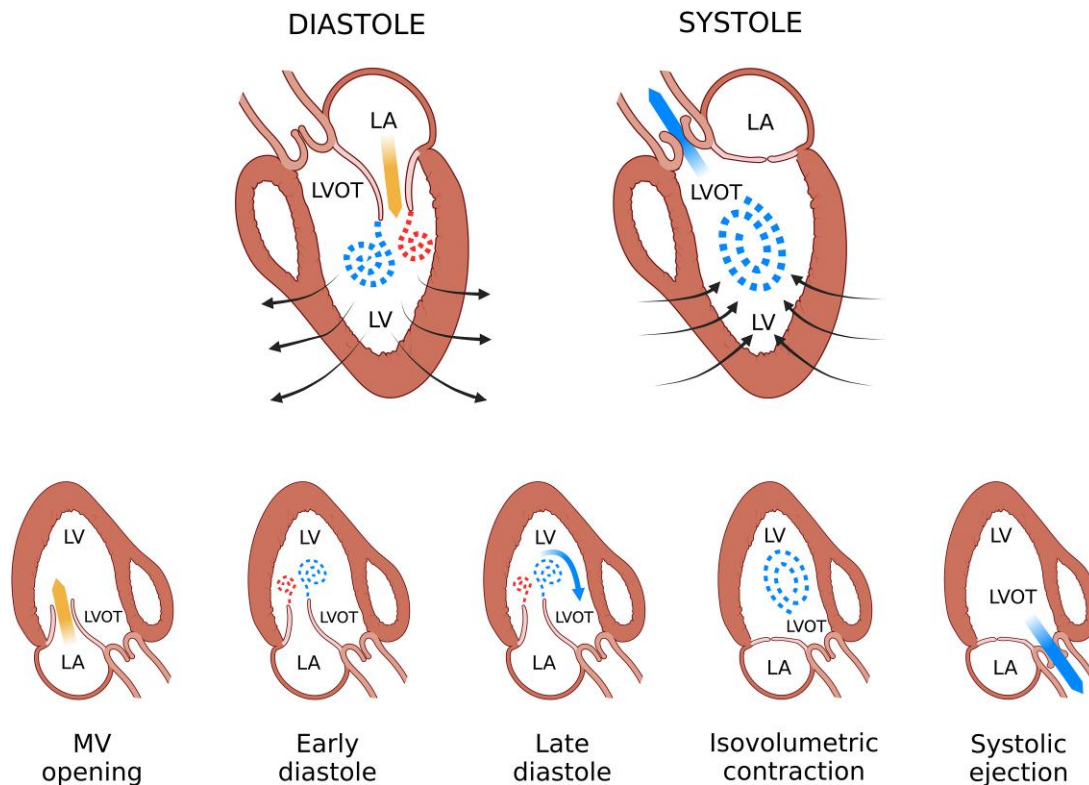


**Figure 2** Normal flow pattern inside the LV cavity in a schematic drawing of the long-axis view. Top left. During the early diastolic filling phase, there are two counter-rotating vortices close to the MV leaflet tips: the greatest one is positioned anteriorly and rotates clockwise, while the smallest one is positioned posteriorly and rotates counterclockwise. Top right. During early systole there is a single vortex rotating clockwise in the LV cavity. Bottom. The process of vortex formation is more detailed from the MV opening to systolic ejection. LA, left atrium; LVOT, left ventricular outflow tract; LV, left ventricle.

appearance of a dominant systolic vortex near the interatrial septum. However, whether this flow pattern is similar in cases of eccentric MR jets directed towards the lateral wall could not be determined. These authors also observed elevated values of tKE in all patients; peak LA tKE occurred consistently at late systole. The LA tKE per heartbeat was significantly and closely related to the MR volume, suggesting that this quantitative measure of flow distortion reflects the severity of MR. This could provide a new perspective in gauging the severity of MR by measuring the energy properties of blood flow in the LA.

In summary, both experimental and clinical research indicate that MR significantly alters LV and LA flow dynamics (Table 2). These alterations include the disruption of organized vortex formation and the introduction of unstructured, turbulent flow patterns with increased kED. Some studies have evidenced that flow alterations inside the LV cavity are plane-dependent, with the antero-posterior plane (corresponding to the echocardiographic apical long-axis view) showing higher velocities and vorticity. LV flow dynamics can also differ in patients with DMR and FMR.

## MV repair

Mitral valve repair (MVR) is the cornerstone treatment for severe MR, due to its ability to preserve the native valve architecture.

Pugliese et al.<sup>18</sup> observed that the blood flow pattern inside the LV cavity was mostly restored by MVR. Whether a triangular resection alone or NeoChord implantation was combined with the annuloplasty

ring, the formation of two counter-rotating vortices was observed during early diastole. A difference from healthy controls was the slightly longer persistence of the posterior vortex during diastole. Two counter-rotating vortices in the LV cavity during early diastole were also reported after transapical off-pump NeoChord implantation.

Al-Wakeel et al.<sup>16</sup> reported that MVR decreased non-normalized mean KE, as well as systolic and early diastolic KE peaks. However, when KE was normalized to LV blood volume, these values became non-significant. Conversely, both non-normalized and normalized late diastolic KE peaks remained at relatively high pre-operative values.

Akiyama et al.<sup>21</sup> observed that following MVR most patients exhibited normal vortex patterns, with the transmitral inflow drifting towards the apex. However, there were two exceptional patients whose post-procedure vortex patterns changed: one underwent PML resection and the other one PML plication. Probably, the rigidity of the PML caused by the resection restricted leaflet opening, directing transmitral inflow towards the antero-septal wall. In these two cases the mitral-septal angle (defined as the angle between the mitral annulus and the antero-septal wall of the LV mid-portion measured during early diastole in the long-axis view) did not exceed 70°, indicating that patients with pre-operative mitral-septal angle  $\leq 70^\circ$  were at risk of having an abnormal vortex. Importantly, kEL was significantly lower in the MVR group compared with those who underwent mitral valve replacement (MVR).

Nakashima et al.<sup>22</sup> after MVR observed diastolic clockwise vortices in all patients. However, these vortices exhibited greater kEL and KP compared with counterclockwise vortices in patients who underwent MVR. Despite

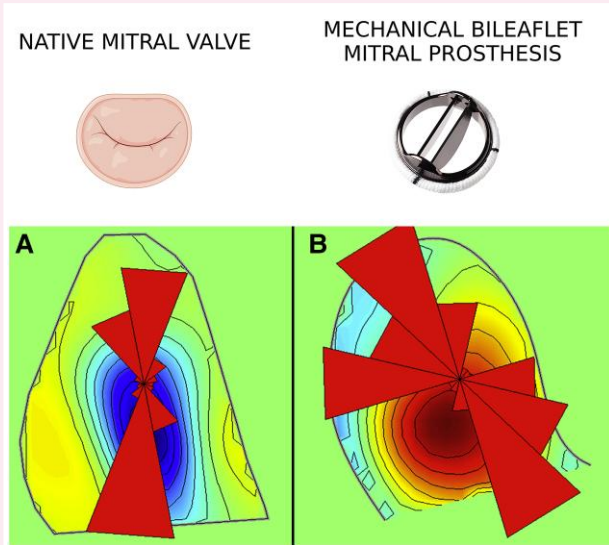


**Figure 3** Intensity-weighted polar histogram representing the distribution and intensity of the LV haemodynamic forces occurring during an entire heartbeat in a normal subject (A) and in a patient with a mechanical mitral prosthesis (B). The LV apical long-axis view is superimposed on the polar map. This polar representation gives a synthetic picture of the overall haemodynamic forces associated with intraventricular blood motion. In the normal subject the haemodynamic forces are aligned along the LV base-apex direction according to the normal emptying-filling process of the LV and there is clockwise rotation of flow. In the polar histogram of the patient with mechanical prosthesis there is a counterclockwise rotation of flow and the distribution of the haemodynamic forces presents significant transverse components.

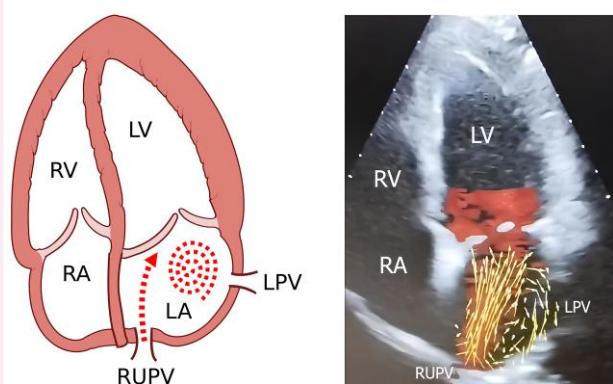


**Figure 4** Normal flow pattern inside the LA cavity. Left. Schematic drawing of a cardiac 4-chamber view. Blood flow entering the LA from the RUPV has a different path compared with that of blood flow entering from the LPV and a vortex develops at the centre of the LA cavity. Right. Colour Doppler apical 4-chamber view obtained using the HyperDoppler technique. The arrows superimposed on the colour Doppler velocity map indicate a vortical flow in the LA cavity. LA, left atrium; LV, left ventricle; RA, right atrium; RV, right ventricle; LPV, left pulmonary vein; RUPV, right upper pulmonary vein.

these differences, the overall diastolic energy efficiency, expressed by the flow energy efficiency ratio (kEL/KP), remained similar between the two vortex types (clockwise and counterclockwise), while a smaller systolic kEL/KP ratio was observed in patients with clockwise vortices.

Yoshida *et al.*<sup>23</sup> reported that in patients with preserved LV ejection fraction (EF) before MVRe, surgery was associated with normal vortex formation, but with elevated kEL and WSS compared with healthy controls. In patients with reduced EF before MVRe, after surgery kEL was the only outlier.

Wang *et al.*<sup>17</sup> showed that in patients with DMR who underwent MVRe, the kEL inside the LV cavity decreased one month after MVRe, although it remained higher compared with normal subjects. In the subgroup of patients who underwent leaflet resection, kEL was higher. No impact on kEL was observed in patients who had extension of leaflet degeneration and implantation of NeoChord.

Morichi *et al.*<sup>24</sup> observed that after MVRe the LV kEL was higher than in the healthy volunteers. Importantly, relatively small annuloplasty rings disturbed the LV flow pattern and caused high kEL.

To evaluate the impact of annuloplasty ring placement on LV intraventricular flow, Witschey *et al.*<sup>25</sup> conducted an animal study and confirmed that post-surgical LV flow dynamics were highly dependent on annuloplasty size. The LV flow dynamics of the smallest ring were characterized by an inflow jet redirected towards the septum. A single, large posterior vortex developed in early diastole, which continued to circulate deep into the apex through late diastole until the beginning of systole, when the blood flowed from the vortex into the LVOT. The anterior vortex was absent.

In summary, while MVRe significantly improves intracardiac flow dynamics with respect to native MR, alterations may persist compared with healthy individuals (Table 3). Residual flow disturbances keep kEL moderately elevated inside the LV cavity. Importantly, the pre-operative mitral-septal angle and some repair techniques, specifically annuloplasty with small rings and leaflet resection in some cases, significantly impact LV flow dynamics.

## The Alfieri stitch

MV edge-to-edge repair, commonly known as the Alfieri stitch after the surgeon who invented it, is a surgical procedure aimed at correcting MR by suturing the free edges of the leaflets. The MV leaflets can be sutured at three different positions: central, lateral, and commissural.

Akiyama *et al.*<sup>26</sup> in a patient who underwent both the Alfieri stitch and aortic valve replacement revealed an abnormal blood flow pattern during diastole (an anterior wall to posterior wall vortex), which was opposite to the normal pre-repair flow pattern. Additionally, the kEL was significantly higher post-repair than during the pre-repair phase. Standard haemodynamic parameters—such as blood pressure, heart rate, and cardiac output—remained within normal ranges.

According to Shi and He,<sup>27</sup> the primary factors implicated in the generation of abnormal vortices following the Alfieri stitch are the suturing technique and configuration. In an *in vitro* model, these authors showed that commissural suturing yielded more physiological flow characteristics, with reduced WSS, closely resembling those of a healthy MV. Conversely, central or lateral suture placements were associated with less favourable haemodynamic profiles. Notably, as the suture length increased in the central position, there was a pronounced deterioration in key flow parameters, including an increase in WSS and kEL, indicating a clear correlation between suture configuration and adverse intraventricular flow patterns. These findings were further supported by a computational fluid dynamics parametric model by Du *et al.*<sup>28</sup> which consistently demonstrated the haemodynamic superiority of commissural suture placement.

The main factors shaping abnormal intracardiac vortex formation after MVRe are summarized in Table 4.

**Table 1** Main properties of intracardiac vortex, energy and haemodynamic forces

Property	Description and explanation	Calculation
VA (cm <sup>2</sup> ) and VAI (dimensionless)	It can be measured at specific point in time or throughout the cardiac cycle (total vortex area). The VAI is the ratio between the total vortex area and the LV area.	VAI = total VA/LV area.
VLI (dimensionless)	It can be measured at specific point in time or throughout the cardiac cycle (total vortex length). The VLI is the ratio between the total vortex length and the LV length.	VLI = total vortex length/LV length.
VDi (dimensionless)	It is the vertical position of the centre of the vortex (the distance of its centre from the mitral annular plane) relative to the LV long-axis.	VDi = distance of vortex centre from LV base/LV long-axis
Vortex circulation (cm <sup>2</sup> /s)	It is the integral of the vorticity inside the vortex, normalized with the LV total vorticity. It may refer to the clockwise (CW) or counterclockwise (CCW) vortex.	Circulation = vortex vorticity/LV total vorticity.
VS or VI (cm <sup>2</sup> /s)	It is the total amount of vortex vorticity. It refers to the sum of the CW and CCW vortex circulation.	VS = CW circulation + CCW circulation.
KE (mj) and KEi (mj/mL)	It is the KE contained in the LV cavity area (in 2D images) or volume (in 3D images). It can be normalized with the LV area/volume, to give average KE and remove dependence from the LV size. The KE of the intraventricular flow depends on blood flow velocity and density.	KE = integral over the LV cavity of $1/2\rho (vx^2 + vy^2 + vz^2)$ , where $vz$ is present only in 3D analysis; $\rho$ is the blood density ( $\rho = 1050 \text{ Kg/m}^3$ ).
Viscous kED or kEL (mW/m or J/m·s) or kEDi (dimensionless).	It is the amount of KE, $\Delta KE$ , dissipated into the heart (by viscous friction) during the cardiac cycle. The total KE dissipation is the value integrated over the entire LV; it can be normalized with the average KE (kEDi) to avoid direct dependence from the LV size.	kEDi = integral over the LV cavity and over the heartbeat of the rate of KE dissipation (double scalar product of deformation and stress tensors).
Flow force angle $\phi$ or flow momentum angle (degrees)	Quantitative parameter describing the orientation of the LV haemodynamic forces, that is, the dominant direction of flow momentum identified by an average angle, that lies between 0° (corresponding to longitudinal forces) and 90° (when forces are transverse). Longitudinally oriented haemodynamic forces (directed along the 'base-to-apex' axis) dominate in the normal LV during both systole and diastole, concordant with the predominant directions of acceleration/deceleration of the LV inflow through the MV and outflow through the aortic valve. In a pathologically asynchronous condition, the haemodynamic forces develop transverse components (generally from the infero-posterior to the antero-septal wall of the LV) and the flow force angle increases.	The angle $\phi$ is obtained by $\sin^2\phi$ by the integral during the heartbeat of $F \times \sin^2\theta$ , normalized by the integral of $F$ , where $F(t)$ and $\theta(t)$ are the magnitude and orientation respect to the LV axis, of the force at every instant during the heartbeat.

CW, clockwise; CCW, counterclockwise; KE, kinetic energy; KEi, kinetic energy index; kED, kinetic energy dissipation; kEDi, kinetic energy dissipation index; kEL, kinetic energy loss; LV, left ventricle; MRI, magnetic resonance imaging; VA, vortex area; VAI, vortex area index; VDi, vortex depth index; VI, vortex intensity; VLI, vortex length index; VS, vortex strength.

## MV replacement

MVR can be performed with either a biological or mechanical prosthesis.

### Bioprosthesis

Pedrizetti et al.<sup>29</sup> in a theoretical study showed that the vortical rotary motion of blood inside the LV cavity can be completely reversed after the implantation of a biological (or mechanical) prosthetic valve (Figure 5). This phenomenon was primarily attributed to the symmetry of the implant. The reversed rotation increased kED and modified the pressure distribution inside the LV cavity.

Pugliese et al.<sup>18</sup> after MVR with a bioprosthesis observed only one vortex distal to the valve during diastole, which had a counterclockwise rotation (opposite to that of healthy controls). The vortex occupied the centre of the LV cavity.

Nakashima et al.<sup>22</sup> noticed that diastolic inflow through mitral bioprosthesis valves collided with the antero-septal wall and then turned towards the apex and sequentially to the posterolateral wall. A main vortex formed in the mid-portion of the LV and was counterclockwise.

Akiyama et al.<sup>21</sup> observed that almost all patients with a mitral bioprosthesis had an abnormal vortex pattern within the LV cavity. The authors speculated that, because the bioprosthetic valves opened in a direction perpendicular to the mitral annular line, this caused the

**Table 2** Summary of the analysed human studies describing flow dynamics inside the left ventricular (LV) cavity in patients with native MR

Study	Imaging technique	Number of patients	MR type	Vortex characteristics	KE and kEL/kED
Al-Wakeel et al. 2015 <sup>16</sup>	4D-flow MRI	10	Severity grade II-III, III and IV; non-ischemic and ischemic MR	Larger fraction of recirculating blood compared with normals. Individual patterns of vortices scattered around LV.	Elevated non-normalized mean KE values; normalized KE values not different from normals.
Filomena et al. 2019 <sup>19</sup>	Echo-PIV	20	Severe FMR	Clockwise rotation of vortex. Vortex area index: $0.41 \pm 0.06$ , intensity index: $-0.55 \pm 0.1$ , flow force angle: $36^\circ \pm 6.2^\circ$ .	kED index: $0.44 \pm 0.27$ .
Obermeier et al. 2022 <sup>15</sup>	4D-flow CCT	2	Severe ischemic MR	No clear ring vortex during diastolic inflow, with unstructured vortical flow inside the LV cavity.	Higher kED values during systole and early diastole compared with normals.
Wang et al. 2022 <sup>17</sup>	VFM	50	DMR	More powerful flow-wall collisions inside the LV cavity.	Diastolic kEL significantly higher compared with controls ( $31.64 \pm 13.05$ vs. $6.29 \pm 1.69$ J/s·m, $P < 0.05$ ).
Pugliese et al. 2023 <sup>18</sup>	VFM	10	Severe DMR and FMR	DMR: Normal diastolic vorticity with two counter-rotating vortices. FMR: Single clockwise vortex during early diastolic filling.	EL 0.51 J/m·s in one patient with DMR and 0.65 J/m·s in one patient with FMR.

CCT, cardiac computed tomography; DMR, degenerative mitral regurgitation; FMR, functional mitral regurgitation; KE, kinetic energy; kED, kinetic energy dissipation; kEL, kinetic energy loss; MRI, magnetic resonance imaging; PIV, particle image velocimetry; VFM, vector flow mapping.

transmitral inflow to direct towards the antero-septal wall. In one exceptional case, the vortex pattern was preserved. In that case, the size of the MV prosthesis was the largest (33 mm), and the mitral-septal angle on transoesophageal echocardiography was the greatest ( $90^\circ$ ). In all other cases, the pre-operative mitral-septal angle was  $< 90^\circ$ . Compared to patients who underwent MVRe, in patients treated with MVR the change in kEL was significantly higher.

Yoshida et al.<sup>23</sup> after bioprosthesis implantation observed in all patients with normal EF before surgery a diastolic counterclockwise vortex inside the LV cavity, with transmitral inflow moving towards the interventricular septum. Among patients with reduced EF, a clockwise vortex occurred in eight cases and a counterclockwise vortex in five patients. Because the inflow through a normal prosthetic MV was perpendicular to the MV annular plane in all cases, this could not be the cause of the different vortex rotation. Instead, the authors suggested that the shape and size of the LV, which alter the mitral-septal angle, are key factors influencing LV blood flow. In particular, when the LV is dilated and more spherical, the mitral inflow perpendicular to the mitral annular plane does not collide with the interventricular septum. In other words, advanced LV remodelling changes the mitral inflow direction from the interventricular septum to the apex and tends to maintain normally directed vortical blood flow in patients with prosthetic MVs and low EF. Another important finding of the study by Yoshida et al.<sup>23</sup> is that in low EF patients, the kEL in the prosthetic MV patients was not significantly different from those who underwent MVRe.

Faludi et al.<sup>30</sup> in concordance with the theoretical results obtained from numerical simulations,<sup>31</sup> observed a quite symmetric vortex ring and a central inflow jet through the mitral bioprosthesis directed towards the apex. With atrial contraction, the same flow pattern was reinforced. At the beginning of systole, the symmetry of the flow pattern was lost; the posterolateral vortex became dominant, and the outflowing blood crossed the previous inflow area again. In the hearts of patients with bioprosthetic valves, parameters of energy dissipation were higher

than in the hearts of healthy subjects. This was explained by the division of the bloodstream into counter-rotating parts, which led to a higher kEL than in the single vortex of a normal heart.

In the study by Faludi et al.<sup>30</sup> the position of the MV prosthesis and LV geometry influenced the flow pattern. One patient had a marked antero-septal position of the bioprosthesis, resulting in an inflow jet directed towards the anterior septum. This jet was then redirected towards the lateral wall by the hypertrophied mid-septum, forming two vortices. These data agree with previous colour Doppler observations by Maire et al.<sup>32</sup> who described unusual flow patterns in patients with an eccentric bioprosthetic valve position. The kEL was particularly high in the patient with altered LV geometry.

In summary, most patients with an MV bioprosthesis exhibit a central, counterclockwise vortex in the LV cavity, with blood flow impacting against the interventricular septum (Table 5). This vortex pattern is markedly different from that observed in healthy controls and is consistently associated with increased kEL; in several studies, kEL was also higher in comparison with patients who underwent MVRe. Factors affecting blood flow dynamics include LV geometric changes observed in LV remodelling, specifically the LV spherical shape, and the marked antero-septal position of the bioprosthesis (Table 4).

## Mechanical prosthesis

MVR can be performed using bileaflet or tilting-disc mechanical valves, although bileaflet valves are preferred today. Mechanical prostheses can be positioned in either anatomical orientation (i.e. with the hinge positions approximating the commissures of the previous native valve) or in an anti-anatomical position.

Several studies indicated that mechanical MV prostheses implanted in an anti-anatomical orientation exhibited pathological vorticity patterns similar to those observed with bioprostheses, specifically a counterclockwise vortex rotation, but with significantly higher

**Table 3** Summary of the analysed human studies describing flow dynamics inside the left ventricular (LV) cavity in patients who underwent MVRe

Study	Imaging technique	Number of patients	Surgical technique	Vortex characteristics	KE and kEL
Al-Wakeel et al. 2015 <sup>16</sup>	4D-flow MRI	6	Modified Paneth-Hetzer posterior annulus shortening annuloplasty, modified Gerbode-Hetzer plasty plication	Incomplete restoration of physiological intracardiac blood flow.	Post-operative decrease of mean KE, systolic and early diastolic KE peaks. No post-operative decrease of late diastolic KE peak.
Akiyama et al. 2017 <sup>21</sup>	VFM	15	Annuloplasty alone ( $n = 2$ ) or with PML resection ( $n = 7$ ), NeoChords ( $n = 4$ ), plication ( $n = 1$ ), cleft suture ( $n = 1$ )	Vortex pattern normal in 13 patients and abnormal in two patients with mitral-septal angle $\leq 70^\circ$ .	kEL change (ELC) smaller than in patients with MV replacement.
Nakashima et al. 2017 <sup>22</sup>	VFM	4	Annuloplasty	Clockwise vortex in the LV mid-portion, similar to mechanical valves in anatomical position.	Systolic EL/EP lower in clockwise than counterclockwise vortex; diastolic EL/EP ratios similar.
Yoshida et al. 2018 <sup>23</sup>	VFM	52 (33 with normal EF, 19 with low EF)	Annuloplasty (with additional repair techniques for DMR)	Clockwise vortex in 91% of patients with preserved EF and in all patients with reduced EF. Higher WSS on ventricular septum in the 9% of patients with counterclockwise vortex.	kEL higher compared with normals and lower compared with patients with valve replacement, both in patients with normal and reduced EF.
Morichi et al. 2022 <sup>24</sup>	4D-flow MRI	14	Semi-rigid partial band ( $n = 7$ ), flexible partial band ( $n = 2$ ), semi-rigid complete ring ( $n = 5$ )	Different vortex flow patterns depending on ring type; small rings disturbed LV flow pattern.	Higher kEL compared with normals [0.65 (0.50–1.15) mW vs. 0.45 (0.38–0.53) mW]. Small rings increased kEL.
Wang et al. 2022 <sup>17</sup>	VFM	50	O-shaped semi-rigid ring, with leaflet resection ( $n = 29$ ) or NeoChords ( $n = 27$ )	In patients with leaflet resection inflow jet tended to collide on the LV wall.	Post-operative decrease of kEL ( $11.33 \pm 3.70$ J/m <sup>3</sup> s vs $31.64 \pm 13.05$ J/m <sup>3</sup> s) but at values higher than normals ( $6.29 \pm 1.69$ J/m <sup>3</sup> s).
Pugliese et al. 2023 <sup>18</sup>	VFM	4	Semi-rigid Simulus annuloplasty ring (three with posterior leaflet resection, one with NeoChord)	Two counter-rotating vortices during early diastole. Longer persistence of posterior vortex compared with normals.	Post-repair kEL values nearly identical to normal values (0.39 J/m <sup>3</sup> s vs. 0.36 J/m <sup>3</sup> s).
		3	Transapical off-pump NeoChord implantation	Two counter-rotating vortices during early diastole.	EL in one patient treated with three pairs of NeoChords for P <sub>2</sub> : 0.41 J/m <sup>3</sup> s

EF, ejection fraction; EL/EP, energy loss/energy pressure; KE, kinetic energy; kEL, kinetic energy loss; MRI, magnetic resonance imaging; MR, mitral regurgitation; PML, posterior mitral leaflet; VFM, vector flow mapping; WSS, wall shear stress.

kEL compared with bioprosthesis-based MVR<sup>8,18,22,30</sup> (Figure 5). Conversely, the placement of a mechanical prosthesis in anatomical position produced contrasting findings. Nakashima et al.<sup>22</sup> found that in patients implanted with a bileaflet mechanical valve, anatomical placement restored near-normal vortex formation, resembling that observed after MVRe, with clockwise rotation of the vortex inside the LV cavity. In contrast, Faludi et al.<sup>30</sup> found that anatomical placement led to significant flow disturbances, characterized by a counterclockwise vortex and high kEL.

In a patient with a single-disc prosthesis, Faludi et al.<sup>30</sup> observed that the majority of the inflow was directed through the larger orifice towards the interventricular septum and then redirected by the hypertrophied septum to form a large clockwise-rotating vortex filling the basal two-thirds of the

LV; they also noted a small counterclockwise-rotating vortex in the anterior apex (Figure 5). Similar to other prosthetic valves, the outflowing blood crossed the previous inflow area. Additionally, parameters of energy dissipation were higher compared with those seen in healthy hearts.

The flow implications of different orientations and types of mechanical prostheses have been evaluated in two animal studies by Mächler et al.<sup>33,34</sup> In the first study,<sup>33</sup> performed with a bileaflet mechanical valve, the anatomical 45° orientation of the valve was shown to produce a more natural and homogeneous washout effect compared with other orientations and anti-anatomical implantation, although there was an increase in inhomogeneous and accelerated local blood velocities compared with pre-operative flow, especially at the apex. In the second study,<sup>34</sup> conducted with a tilting-disc valve, the anatomical

**Table 4** Main factors shaping abnormal intracardiac vortex formation after MV surgery

Determinant factors	Consequences
<b>MV repair</b>	
Mitral-septal angle	In MV repair, the pre-operative mitral-septal angle $\leq 70^\circ$ is a risk factor for an abnormal vortex pattern, favouring transmitral inflow motion towards the antero-septal wall.
PML resection	In MV repair with PML resection, the rigidity of the leaflet restricts its motion and valve opening, thus transmitral inflow seemed to stream towards the antero-septal wall.
Annular size	In MV repair with annuloplasty, a small annular size is associated with abnormal intracardiac vortex formation and therefore higher KE loss.
Site of stitch	In MV repair with the Alfieri stitch, central stitch increases wall shear stress and KE loss, while commissural suturing yields more physiological flow characteristics.
<b>MV replacement</b>	
Prosthesis orientation	In MV replacement with a prosthesis in anti-anatomical position, anticlockwise vortex flow pattern generates higher KE loss.
Prosthesis antero-septal position	If a prosthesis is in a marked antero-septal position, this results in a transmitral inflow jet directed towards the anterior septum.

PML, posterior mitral leaflet; KE, kinetic energy.

orientation again demonstrated a flow pattern closely resembling normal LV physiology. Conversely, when the valve was placed in an anti-anatomical orientation, significant flow disturbances were observed, including increased turbulence and altered flow patterns.

A few additional *in vitro*<sup>35</sup> and *in silico*<sup>36</sup> studies evaluating implanted mechanical MV prostheses simulations reported substantially similar findings, with some discrepancies that may be explained by differences in study design and models employed.

In summary, the effects of mechanical MV prostheses on intraventricular flow dynamics mainly depend on the orientation (anatomical vs. anti-anatomical) and type of prosthesis, with the tilting-disc valve exhibiting a distinctive flow behaviour (Table 5).

## Transcatheter approaches

Percutaneous interventions, such as transcatheter edge-to-edge repair (TEER) utilizing devices like the MitraClip and transcatheter MV replacement (TMVR), have expanded treatment options for patients with severe MR.

### Transcatheter edge-to-edge repair

Gooden *et al.*<sup>13</sup> in an *in vitro* model observed that MitraClip deployment determined markedly abnormal vorticity patterns characterized by two divergent jets with reduced velocity, elevated RSS, and multiple high-shear regions in the chamber acting as the LV, which collectively contributed to increased kEL.

Jeyhani *et al.*<sup>37</sup> in another *in vitro* study simulating MV TEER, observed that vortex development in the LV cavity during diastole was significantly different than after repair. TEER increased the amplitude of RSS and VSS, as well as the number of high-shear regions in the LV cavity.

Hu *et al.*<sup>38</sup> in a study based on computational simulations of flow dynamics in MV TEER, found that the intraventricular flow pattern was unique, characterized by two jets and two vortex rings; the large anterior vortex did not clearly exist after rapid LV filling, and kEL increased with the decrease of the total orifice area after TEER. The high kEL was caused by the two high-speed jets, which were deflected laterally and impinged upon the LV wall.

Pugliese *et al.*<sup>18</sup> in patients implanted with a MitraClip, showed, during diastole, multiple vortices without the formation of the typical main clockwise vortex occupying the centre of the LV cavity. In systole, haemodynamic forces were partially restored along the LV longitudinal axis, from the apex to the LVOT. In the LA, an incomplete pair of counter-rotating vortices was noted due to the residual MR.

Filomena *et al.*<sup>19</sup> found that, in patients who underwent MitraClip implantation, the vortex area and the intensity index decreased after the procedure. Conversely, a significant increase in the kED index and flow force angle was observed, with the appearance of transverse intraventricular thrusts from the infero-posterior to the antero-septal LV wall. None of the patients exhibited a reversal in the vortical fluid motion in the LV cavity.

Overall, the MitraClip implantation produced similar detrimental effects on LV flow dynamics as the Alfieri stitch with a central suture (shear stress and kEL increase and inefficient blood flow dynamics inside the LV cavity) (Table 6).

## Transcatheter MVR

Hatoum *et al.*<sup>39</sup> evaluated in an *in vitro* study a Caisson MV of size 36A implanted in the mitral position of a left heart simulator. The authors assessed flow turbulence by calculating the RSS and VSS and observed that the overall levels of RSS did not exceed 100 Pa, and the VSS did not exceed 10 Pa, indicating a potential low risk of platelet activation or red blood cell destruction leading to haemolysis.

Pugliese *et al.*<sup>18</sup> using VFM, evaluated three patients who were implanted with a Tendyne prosthesis. During early filling, the formation of two typical counter-rotating vortices inside the LV cavity was observed, with the larger vortex located below the AML pushing back the blood flow and redirecting it towards the LVOT.

Although very preliminary, the results of these studies suggest that TMVR may lead to an LV flow pattern that is close to the normal behaviour and holds the potential for favourable hemodynamics with a low degree of turbulence (Table 6).

## The issue of MV symmetry

The implantation of a MV prosthesis, whether through a surgical or transcatheter approach, may disrupt the natural asymmetric configuration of the native MV. Given the importance of preserving the native MV asymmetry to sustain physiological blood flow, research efforts focused on developing surgical and interventional strategies to maintain this asymmetry during MVR.

Colia and Pedrizzetti<sup>40</sup> employed numerical simulations to identify the optimal asymmetry parameters for surgical interventions. Vukićević *et al.*<sup>41</sup> designed an original, homemade asymmetric MV prototype characterized by two unequal leaflets and an enlarged central orifice, which successfully achieved nearly physiological flow parameters. Scorsin *et al.*<sup>42</sup> developed a model of a transcatheter MV prosthesis specifically engineered to maintain native asymmetry, aiming to support physiological LV vortex patterns. Custom MV prostheses featuring D-shaped rings designed to mimic the natural valve geometry were tested in two *in vitro* studies by Okafor *et al.*<sup>43</sup> and Tan *et al.*<sup>44</sup> successfully achieving a more natural vortex pattern and a reduction in kEL.

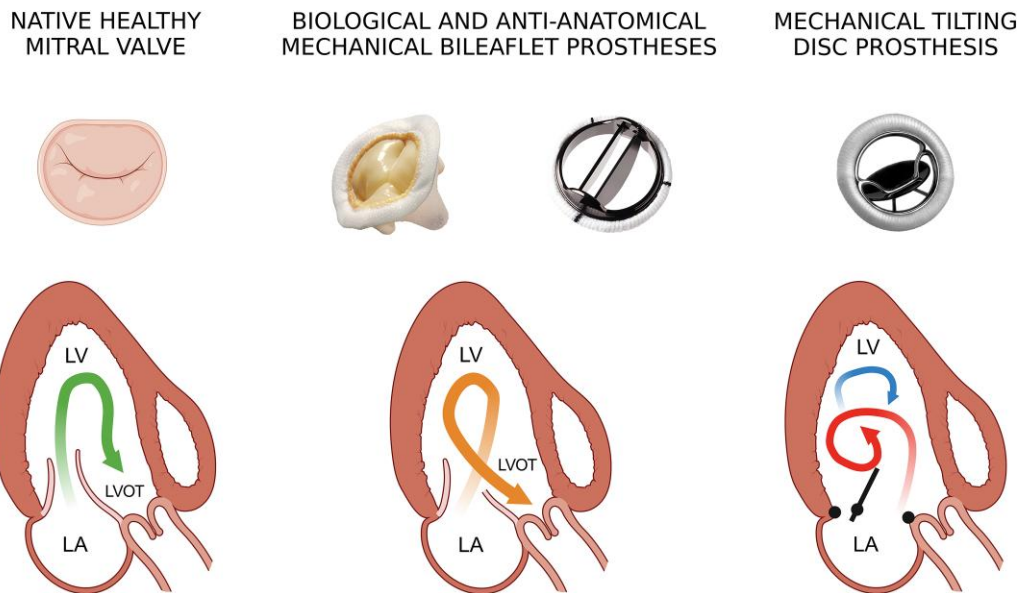


**Figure 5** Blood flow patterns inside the LV cavity are depicted in a schematic of the cardiac long-axis view for a normal MV, a biological trileaflet or mechanical bileaflet valve in anti-anatomical position, and a mechanical tilting disc valve. The figure is based on the results of Pedrizzetti et al.<sup>29</sup> and Faludi et al.<sup>30</sup>. LA, left atrium; LVOT, left ventricular outflow tract; LV, left ventricle.

## Implications of abnormal intracardiac vorticity

Blood flow and myocardial walls form a cohesive unit essential for normal cardiac function, as the IVPGs are transmitted from the LV walls to other segments through incompressible blood. Deviations of IVPGs from the normal base-apex direction generate transverse haemodynamic forces (Figure 3) that alter myocardial wall stress. Although the mechanisms of LV remodelling have not been fully elucidated, a local increase in wall stress is considered the main pathway leading to LV remodelling.<sup>6</sup> More specifically, abnormal wall stress can be recognized by LV mechanoreceptors, triggering intracellular signalling pathways that ultimately lead to changes in myocyte gene expression, potentially determining or sustaining adverse remodelling in the entire LV.

Another consequence of disrupted intracardiac flow within the LV cavity, primarily due to changes in the direction of blood flow impinging on the LV walls, is the increase of kEL, which generates the need for greater mechanical energy expenditure to maintain haemodynamics and cardiac output. This adaptation elevates metabolic demands and impairs mechano-electric coupling, further driving pathological remodelling and exacerbating the progression of heart failure.

Abnormal intracavitary flow may increase the risk of thromboembolism. Elevated VSS and RSS related to turbulence enhance platelet aggregation through activation of the von Willebrand factor.<sup>45</sup> Post-surgical interventions, such as heart valve replacement, can exacerbate pathological vorticity, creating a pro-thrombotic environment that necessitates long-term anticoagulation therapy to mitigate thromboembolic complications. Finally, the abnormal flow caused by the implantation of a heart valve leads to non-physiological forces on red blood cells, which may cause rupture (haemolysis).<sup>46</sup>

The impact of perturbations of intracardiac flow dynamics is schematically represented in the Figure 6.

## Potential impact on patient management

Evaluation of intracardiac flow dynamics (in addition to haemodynamic evaluations, such as MR volume, LV volume overload and estimation of LV filling pressure) can potentially reshape the management of MR patients by enhancing diagnostic precision, guiding surgical strategies, and informing post-operative care. For example, incorporating LV flow analysis into pre-operative planning enables identification of high-risk features, such as unfavourable mitral-septal angles (Table 4), which are associated with abnormal vortex formation. Post-operative monitoring by intracardiac flow dynamics analysis can quantify residual turbulence, elevated shear stress, and increased kEL, guiding interventions to prevent long-term complications. These insights offer a pathway to precision medicine in MR, optimizing surgical and interventional outcomes while reducing the burden of adverse cardiac remodelling.

## Gaps in information

There are a number of unsolved issues about intracardiac flow dynamics in the field of MR.

First, most of the information refers to severe MR. There is a lack of information about intracardiac flow dynamics (inside the LV and LA cavity) in patients with mild and moderate MR and their progression over time. Additionally, so far only pure MR cases have been studied, leading to a lack of knowledge about combined MR with aortic regurgitation, as well as combined mitral stenosis and MR. Evaluations in vitro show that paravalvular leaks in patients with transcatheter aortic valve replacement led to abnormal vortex formation, interfering with the natural advancement of transmitral flow and negatively affecting the LV fluid dynamics.<sup>47</sup>

Second, it is unknown whether the findings reported in normal sinus rhythm are consistent in patients with irregular rhythms, for example, if atrial fibrillation coexists. Initial observations with 4D-flow MRI show that LA peak velocity and vorticity are reproducible and temporally stable

**Table 5 Summary of the analysed human studies describing flow dynamics inside the left ventricular (LV) cavity in patients who underwent MV replacement**

Study	Imaging technique	Number of patients	Surgical technique	Vortex characteristics	KE and kEL
<b>Biological prostheses</b>					
Faludi <i>et al.</i> 2010 <sup>30</sup>	Echo-PIV	4	Bioprosthesis	At early diastole, a central jet is directed towards the apex, with symmetric vortex ring; with atrial contraction, this flow pattern is reinforced. At the beginning of systole, the symmetry of the flow pattern is lost and the dominant part rotates counterclockwise (opposite than normal).	Increased kEL due to the two counter-rotating symmetric vortices compared with normals.
Akiyama <i>et al.</i> 2017 <sup>21</sup>	VFM	17	14 Mosaic porcine, 2 EPIC, 1 CEP Magna bioprotheses	Abnormal vortex patterns, generally with flow collision with the antero-septal wall and counterclockwise vortex rotation.	kEL change (ELC) higher than in patients with MV repair (196.6% vs. 71.9%, $P = 0.009$ ).
Nakashima <i>et al.</i> 2017 <sup>22</sup>	VFM	3	Carpentier-Edwards Perimount pericardial bioprotheses	Counterclockwise vortex in the LV mid-portion, similar to mechanical valves in anti-anatomical position. Smaller apical vortex due to flexible leaflets.	Systolic EL/EP ratio higher in counterclockwise than clockwise vortex; diastolic EL/EP ratios similar.
Yoshida <i>et al.</i> 2018 <sup>23</sup>	VFM	29	Bioprotheses (normal LV EF in 16 patients; low LV EF in 13 patients)	Normal LV EF: LV inflow towards the interventricular septum and counterclockwise vortex. Low LV EF: clockwise vortex (8 cases) or counterclockwise (5 cases).	Normal LV EF: kEL significantly higher compared with MVRe patients. Low LV EF: kEL not significantly different from MVRe.
Pugliese <i>et al.</i> 2023 <sup>18</sup>	VFM	3	Bioprotheses	Single diastolic vortex in the LV mid-cavity, with counterclockwise rotation.	EL in one patient with a Medtronic Mosaic 33 valve: 0.48 J/m <sup>3</sup>
<b>Mechanical prostheses</b>					
Faludi <i>et al.</i> 2010 <sup>30</sup>	Echo-PIV	5	Mechanical bileaflet valves in anatomical position	Counterclockwise vortex	High kEL compared with controls and anti-anatomical position.
		1	Mechanical single-disc valve	Large clockwise vortex filling basal two-thirds of LV; small counterclockwise vortex in the anterior apex.	Higher energy dissipation parameters than normals.
Nakashima <i>et al.</i> 2017 <sup>22</sup>	VFM	11	Mechanical bileaflet valves, nine in anti-anatomical position and two in anatomical position	Anatomical position: clockwise vortex rotation. Anti-anatomical position: counterclockwise vortex rotation.	Systolic EL/EP ratio higher in counterclockwise than clockwise vortex; diastolic EL/EP ratios similar.
Yoshida <i>et al.</i> 2018 <sup>23</sup>	VFM	8	Mechanical prostheses (normal LV EF in three patients; low LV EF in five patients)	Normal LV EF: LV inflow towards the interventricular septum and counterclockwise vortex. Low LV EF: clockwise vortex (1 case) or counterclockwise (4 cases).	kEL analysis included in the group with biological prostheses (see above).
Pugliese <i>et al.</i> 2023 <sup>18</sup>	VFM	2	Mechanical prostheses in anti-anatomical orientation	Single diastolic vortex in the LV mid-cavity, with counterclockwise rotation.	EL in one patient with a Carbomedics Corcym 29 valve: 0.55 J/m <sup>3</sup>

CEP, Carpentier-Edwards Perimount; Echo-PIV, echocardiographic particle image velocimetry; EF, ejection fraction; KE, kinetic energy; kEL, kinetic energy loss; MV, mitral valve; MVR, mitral valve replacement; MVRe, mitral valve repair; VFM, vector flow mapping.

**Table 6** Summary of the analysed human studies describing flow dynamics inside the left ventricular (LV) cavity in patients who underwent percutaneous interventions on the mitral valve

Study	Imaging technique	Number of patients/ model	Interventional technique	Vortex characteristics	KE and kEL
Filomena et al. 2019 <sup>19</sup>	Echo-PIV	20	TEER (MitraClip)	Reduced vortex area and intensity index; no reversal in vortical fluid motion; altered IVPGs with transverse thrusts in the LV cavity.	Increased kED index ( $0.62 \pm 0.42$ vs. $0.44 \pm 0.27$ , $P = 0.018$ ) and flow force angle ( $41 \pm 8.6$ vs. $36 \pm 6.2$ , $P = 0.036$ )
Pugliese et al. 2023 <sup>18</sup>	VFM	2	TEER (MitraClip)	Multiple vortices without forming the typical main clockwise vortex; haemodynamic forces partially restored during systole; incomplete pair of counter-rotating vortices in the LA.	Increased kED. EL in one patient with two MitraClips: $0.67 \text{ J/m}^3$
		3	TMVR (Tendyne prosthesis)	Two counter-rotating vortices inside the LV cavity during early filling, with the major clockwise vortex beneath AML.	Low turbulence. EL in one patient with a Tendyne LP 33S: $0.47 \text{ J/m}^3$

Echo-PIV, echocardiographic particle image velocimetry; IVPGs, intraventricular pressure gradients; KE, kinetic energy; kED, kinetic energy dissipation; kEDi, kinetic energy dissipation index; kEL, kinetic energy loss; LA, left atrium; LVOT, left ventricular outflow tract; TEER, transcatheter edge-to-edge repair; TMVR, transcatheter mitral valve replacement; VFM, vector flow mapping.

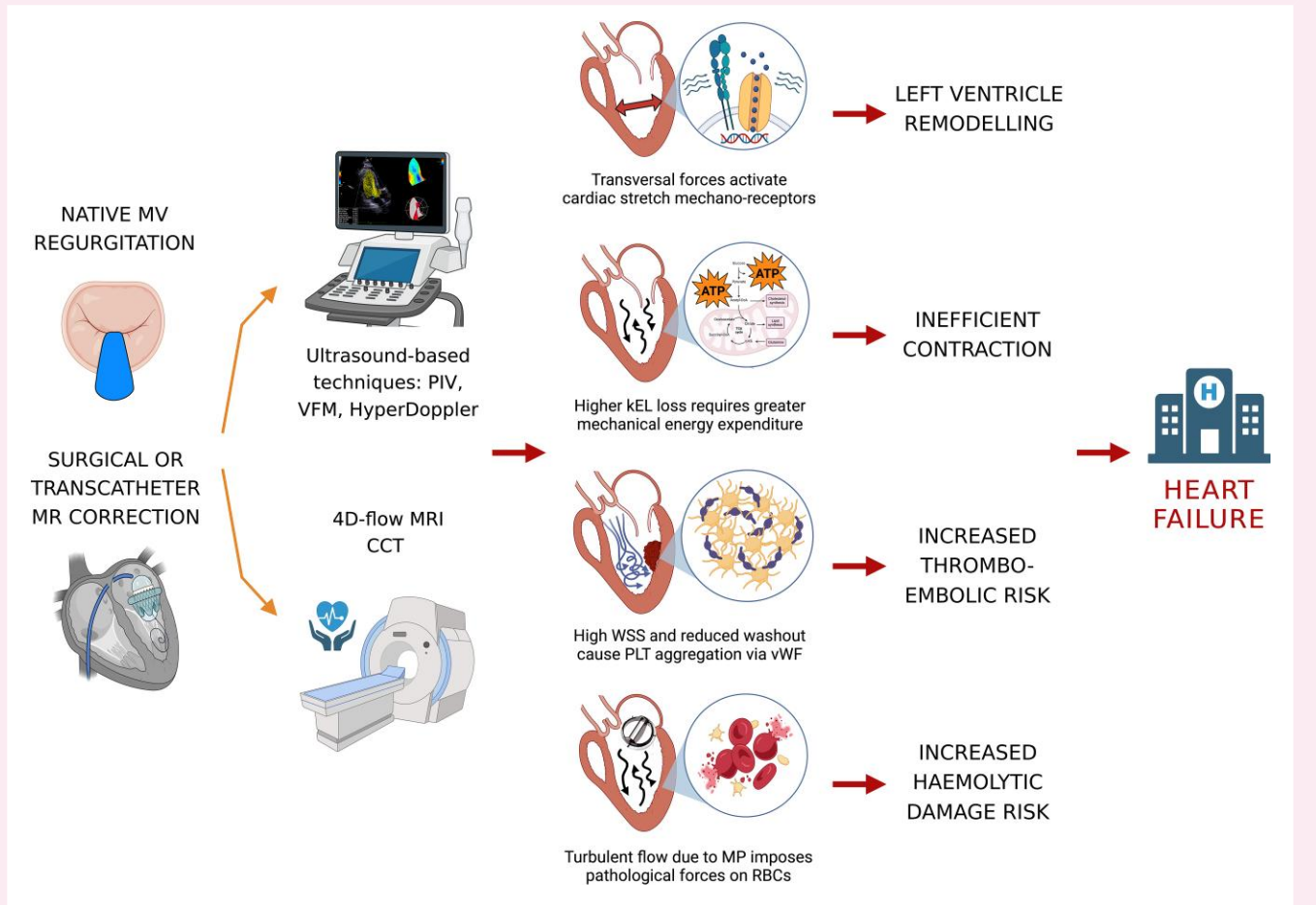


**Figure 6** Negative effects of MR, surgical and transcatheter correction of the MV disease on left ventricular remodelling and contraction, thrombo-embolic risk, and haemolysis risk. CT, computed tomography; 4D-flow MRI, four-dimensional-flow magnetic resonance imaging; kEL, kinetic energy loss; PIV, particle imaging velocimetry; PLT, platelet; MR, mitral regurgitation; MV, mitral valve; RBCs, red blood cells; VFM, vector flow mapping; vWF, von Willebrand factor; WSS, wall shear stress.

flow biomarkers and are robust to changes in heart rate, blood pressure, and differences in heart rhythm.<sup>48</sup> Further investigations are needed.

Third, it remains unclear whether the reversal of maladaptive myocardial responses to severe MR can be predicted by restoration of intracardiac flow dynamics after treatment, as previously demonstrated with cardiac resynchronization therapy devices. Specifically, Pedrizzetti *et al.*<sup>49</sup> observed that changes in electrical activation following cardiac resynchronization therapy implantation alter the orientation of the haemodynamic forces inside the LV cavity. Long-term reverse LV remodelling correlates with the degree of realignment of flow force momentum: the more longitudinal it becomes, the greater the observed reduction in end-systolic volume at follow-up.

Finally, in current clinical investigations on intracardiac flow dynamics in patients with MR and those who underwent percutaneous and surgical correction, the number of patients is limited and the duration of follow-up is inadequate to draw reliable conclusions. Multicenter studies with large sample sizes and long-term follow-up are essential to confirm initial observations.

## Conclusion

MR significantly alters blood flow patterns in the LV and LA cavities, contributing to a loss of vortex organization and an increase in turbulence, which adversely affects cardiac function and the mechanical energy required to maintain cardiac output. Advanced imaging techniques, especially based on ultrasound and MRI, have enabled the quantitative characterization of these alterations.

Compared to MVR, MVRe can restore intracardiac flow dynamics, although some abnormalities persist. Transcatheter procedures, such as the MitraClip, introduce disturbances in flow patterns, which might explain reported complications, such as adverse remodelling and potential thrombus formation.

Future research should focus on the role of intracardiac flow dynamics analysis to guide the management of MR patients and intervention modalities that preserve or restore the anatomical asymmetry of the MV to support physiological flow patterns and optimize clinical outcomes.

**Conflict of interest:** None declared.

## Funding

None declared.

## Data availability

No new data were generated or analysed in support of this research.

## Lead author biography



Donato Mele, MD, FESC, Associate Professor of Cardiology, Department of Cardiac Thoracic Vascular Sciences and Public Health, University of Padova, Italy. Head of the Echocardiographic Laboratory, Cardiology Unit, University Hospital of Padova, Italy.

## References

- Mele D, Smarrazzo V, Pedrizzetti G, Capasso F, Pepe M, Severino S, *et al.* Intracardiac flow analysis: techniques and potential clinical applications. *J Am Soc Echocardiogr* 2019; **32**:319–32.
- Mele D, Smarrazzo V, Pedrizzetti G, Bertini M, Ferrari R. Intracardiac flow analysis in cardiac resynchronization therapy: a new challenge? *Echocardiography* 2019; **36**: 1919–29.
- Fiorencis A, Pepe M, Smarrazzo V, Martini M, Severino S, Pergola V, *et al.* Noninvasive evaluation of intraventricular flow dynamics by the HyperDoppler technique: first application to normal subjects, athletes, and patients with heart failure. *J Clin Med* 2022; **11**:2216.
- Lantz J, Gupta V, Henriksson L, Karlsson M, Persson A, Carlhäll C-J, *et al.* Intracardiac flow at 4D CT: comparison with 4D flow MRI. *Radiology* 2018; **289**:51–8.
- Elbaz MSM, Calkoen EE, Westenberg JJM, Lelieveldt BPF, Roest AAW, van der Geest RJ. Vortex flow during early and late left ventricular filling in normal subjects: quantitative characterization using retrospectively-gated 4D flow cardiovascular magnetic resonance and three-dimensional vortex core analysis. *J Cardiovasc Magn Reson* 2014; **16**:78.
- Pedrizzetti G, La Canna G, Alfieri O, Tonti G. The vortex—an early predictor of cardiovascular outcome? *Nat Rev Cardiol* 2014; **11**:545–53.
- Kilner PJ, Yang G-Z, Wilkes AJ, Mohiaddin RH, Firmin DN, Yacoub MH. Asymmetric redirection of flow through the heart. *Nature* 2000; **404**:759–61.
- Sekine T, Nakaza M, Matsumoto M, Ando T, Inoue T, Sakamoto S-I, *et al.* 4D flow MR imaging of the left atrium: what is non-physiological blood flow in the cardiac system? *Magn Reson Med* 2022; **21**:293–308.
- Fyrenius A, Wigström L, Ebberts T, Karlsson M, Engvall J, Bolger AF. Three dimensional flow in the human left atrium. *Heart* 2001; **86**:448–55.
- Dyverfeldt P, Kvitting JE, Carlhäll CJ, Boano G, Sigfridsson A, Hermansson U, *et al.* Hemodynamic aspects of mitral regurgitation assessed by generalized phase-contrast MRI. *Magn Reson Imaging* 2011; **33**:582–8.
- Mele D, Beccari R, Pedrizzetti G. Effect of aging on intraventricular kinetic energy and energy dissipation. *J Cardiovasc Dev Dis* 2023; **10**:308.
- Aimo A, Panichella G, Fabiani I, Garofalo M, Fanizzi AI, Ragagnin M, *et al.* Assessing cardiac mechanics through left ventricular haemodynamic forces. *Eur Heart J—Imaging Methods Pract* 2024; **2**:qyae077.
- Gooden SC-M, Hatoum H, Boudoulas KD, Vannan MA, Dasi LP. Effects of MitraClip therapy on mitral flow patterns and vortex formation: an in vitro study. *Ann Biomed Eng* 2022; **50**:680–90.
- Pilla G, Levack M, Mcgarvey J, Hwuang E, Zsido G, Gorman J, *et al.* Alterations in intracardiac flow patterns affect mitral leaflets dynamics in a model of ischemic mitral regurgitation. *Cardiovasc Eng Tech* 2021; **12**:640–50.
- Obermeier L, Vellguth K, Schlieff A, Tautz L, Bruening J, Knosalla C, *et al.* CT-Based simulation of left ventricular hemodynamics: a pilot study in mitral regurgitation and left ventricle aneurysm patients. *Front Cardiovasc Med* 2022; **9**:828556.
- Al-Wakeel N, Fernandes JF, Amiri A, Siniawski H, Goubergrits L, Berger F, *et al.* Hemodynamic and energetic aspects of the left ventricle in patients with mitral regurgitation before and after mitral valve surgery. *Magn Reson Imaging* 2015; **42**:1705–12.
- Wang Y, Li Y, Cui C, Ge Z, Liu Y, Hu Y, *et al.* Role of vector flow mapping in evaluating left ventricular diastolic flow dynamics in patients who underwent mitral valve repair for degenerative mitral regurgitation. *Rev Cardiovasc Med* 2022; **23**:301.
- Pugliese NR, Colli A, Falcetta G, Del Punta L, Puccinelli C, Fiocco A, *et al.* Flow dynamic assessment of native mitral valve, mitral valve repair and mitral valve replacement using vector flow mapping intracardiac flow dynamic in mitral valve regurgitation. *Front Cardiovasc Med* 2023; **10**:1047244.
- Filomena D, Cimino S, Maestrini V, Cantisani D, Petronilli V, Mancone M, *et al.* Changes in intraventricular flow patterns after MitraClip implant in patients with functional severe mitral regurgitation. *J Am Soc Echocardiogr* 2019; **32**:1250–3.
- Cimino S, Pedrizzetti G, Tonti G, Canali E, Petronilli V, De Luca L, *et al.* In vivo analysis of intraventricular fluid dynamics in healthy hearts. *Eur J Mech B Fluids* 2012; **35**:40–6.
- Akiyama K, Nakamura N, Itatani K, Naito Y, Kinoshita M, Shimizu M, *et al.* Flow-dynamics assessment of mitral-valve surgery by intraoperative vector flow mapping. *Interact Cardiovasc Thorac Surg* 2017; **24**:869–75.
- Nakashima K, Itatani K, Kitamura T, Oka N, Horai T, Miyazaki S, *et al.* Energy dynamics of the intraventricular vortex after mitral valve surgery. *Heart Vessels* 2017; **32**:1123–9.
- Yoshida S, Miyagawa S, Fukushima S, Yoshikawa Y, Hata H, Saito S, *et al.* Cardiac function and type of mitral valve surgery affect postoperative blood flow pattern in the left ventricle. *Circ J* 2018; **83**:130–8.
- Morichi H, Itatani K, Yamazaki S, Numata S, Nakaji K, Tamaki N, *et al.* Influences of mitral annuloplasty on left ventricular flow dynamics assessed with 3-dimensional cine phase-contrast flow magnetic resonance imaging. *J Thorac Cardiovasc Surg* 2022; **163**:947–59.
- Witschey WRT, Zhang D, Contijoch F, McGarvey JR, Lee M, Takebayashi S, *et al.* The influence of mitral annuloplasty on left ventricular flow dynamics. *Ann Thorac Surg* 2015; **100**: 114–21.

26. Akiyama K, Itatani K, Naito Y, Kinoshita M, Shimizu M, Hamaoka S, et al. Vector flow mapping and impaired left ventricular flow after the alferi stitch. *J Cardiothorac Vasc Anesth* 2017;**31**:211–4.
27. Shi L, He Z. Hemodynamics of the mitral valve under edge-to-edge repair: an in vitro steady flow study. *J Biomech Eng* 2009;**131**:051010.
28. Du D, Jiang S, Wang Z, Hu Y, He Z. Effects of suture position on left ventricular fluid mechanics under mitral valve edge-to-edge repair. *Biomed Mater Eng* 2014;**24**:155–61.
29. Pedrizzetti G, Domenichini F, Tonti G. On the left ventricular vortex reversal after mitral valve replacement. *Ann Biomed Eng* 2010;**38**:769–73.
30. Faludi R, Szulik M, D'hooge J, Herijgers P, Rademakers F, Pedrizzetti G, et al. Left ventricular flow patterns in healthy subjects and patients with prosthetic mitral valves: an in vivo study using echocardiographic particle image velocimetry. *J Thorac Cardiovasc Surg* 2010;**139**:1501–10.
31. Pedrizzetti G, Domenichini F. Nature optimizes the swirling flow in the human left ventricle. *Phys Rev Lett* 2005;**95**:108101.
32. Maire R, Ikram S, Odemuyiwa O, Groves PH, Lo SV, Banning AP, et al. Abnormalities of left ventricular flow following mitral valve replacement: a colour flow Doppler study. *Eur Heart J* 1994;**15**:293–302.
33. Machler H, Perthel M, Reiter G, Reiter U, Zink M, Bergmann P, et al. Influence of bileaflet prosthetic mitral valve orientation on left ventricular flow? An experimental in vivo magnetic resonance imaging study. *Eur J Cardiothorac Surg* 2004;**26**:747–53.
34. Mächler H, Reiter G, Perthel M, Reiter U, Bergmann P, Zink M, et al. Influence of a tilting prosthetic mitral valve orientation on the left ventricular flow—an experimental in vivo magnetic resonance imaging study. *Eur J Cardiothorac Surg* 2007;**32**:102–7.
35. Querzoli G, Fortini S, Cenedese A. Effect of the prosthetic mitral valve on vortex dynamics and turbulence of the left ventricular flow. *Physics of Fluids* 2010;**22**:041901.
36. Su B, Kabinejadian F, Phang HQ, Kumar GP, Cui F, Kim S, et al. Numerical modeling of intraventricular flow during diastole after implantation of BMHV. *PLoS ONE* 2015;**10**:e0126315.
37. Jeyhani M, Shahriari S, Labrosse M. Experimental investigation of left ventricular flow patterns after percutaneous edge-to-edge mitral valve repair. *Artif Organs* 2018;**42**:516–24.
38. Hu Y, Shi L, Parameswaran S, Smirnov S, He Z. Left ventricular vortex under mitral valve edge-to-edge repair. *Cardiovasc Eng Tech* 2010;**1**:235–43.
39. Hatoum H, Askegaard G, Iyer R, Dasi LP. Atrial and ventricular flows across a transcatheter mitral valve. *Interact Cardiovasc Thorac Surg* 2021;**33**:1–9.
40. Collia D, Pedrizzetti G. The influence of mitral valve asymmetry for an improved choice of valve repair or replacement. *Fluids* 2022;**7**:293.
41. Vukićević M, Fortini S, Querzoli G, Espa S, Pedrizzetti G. Experimental study of an asymmetric heart valve prototype. *Eur J of Mech B/Fluids* 2012;**35**:54–60.
42. Scorsin M, Andreas M, Corona S, Guta AC, Aruta P, Badano LP. Novel transcatheter mitral prosthesis designed to preserve physiological ventricular flow dynamics. *Ann Thorac Surg* 2022;**113**:593–9.
43. Okafor IU, Santhanakrishnan A, Raghav VS, Yoganathan AP. Role of mitral Annulus diastolic geometry on intraventricular filling dynamics. *J Biomech Eng* 2015;**137**:121007.
44. Tan SG-D, Kim S, Hon JKF, Leo HL. A D-shaped bileaflet bioprosthesis which replicates physiological left ventricular flow patterns. *PLoS ONE* 2016;**11**:e0156580.
45. Hung TC, Hochmuth RM, Joist JH, Suter SP. Shear-induced aggregation and lysis of platelets. *Trans Am Soc Artif Intern Organs* 1976;**22**:285–91.
46. Kameneva MV, Burgreen GW, Kono K, Repko B, Antaki JF, Umezumi M. Effects of turbulent stresses upon mechanical hemolysis: experimental and computational analysis. *ASAIO J* 2004;**50**:418–23.
47. Morisawa D, Falahatpisheh A, Avenatti E, Little SH, Kheradvar A. Intraventricular vortex interaction between transmitral flow and paravalvular leak. *Sci Rep* 2018;**8**:15657.
48. Spartera M, Pessoa-Amorim G, Stracquadanio A, Von Ende A, Fletcher A, Manley P, et al. Left atrial 4D flow cardiovascular magnetic resonance: a reproducibility study in sinus rhythm and atrial fibrillation. *Cardiovasc Magn Reson* 2021;**23**:29.
49. Pedrizzetti G, Martiniello AR, Bianchi V, D'Onofrio A, Caso P, Tonti G. Changes in electrical activation modify the orientation of left ventricular flow momentum: novel observations using echocardiographic particle image velocimetry. *Eur Heart J Cardiovasc Imaging* 2016;**17**:203–9.